Low Loss THz Window

Armin Wagner-Gentner, K. Jacobs, U.U. Graf, and D. Rabanus
KOSMA, 1.Physikalisches Institut
University of Cologne, Germany
Email: wagner@ph1.uni-koeln.de

***Abstract*—This paper presents a method how to manufacture a low loss window applicable for THz frequencies. The window is made out of high resistivity silicon ($3k\Omega cm$, $n = 3.42$ and $\alpha = 0.1/cm$). Reflective loss due to the impedance mismatch between the substrate and free space is overcome by etching (Bosch-process) rectangular grooves of depth $\lambda/4$ into the substrate as an antireflection (AR) layer. Simulation of the AR-layer was done by using a transmission line analogue and the *Scatter*-program written by R. Padman. FTS measurements yield a transmittance greater than 96% at 2.1 THz and a bandwitdh of 400 GHz (1.9-2.3THz) with 90% transmission.**

I. Introduction

In the THz range, standard polymer windows (e.g. HDPE, Mylar) have high absorption. Conversely, substrates transmitting THz radiation (e.g. quartz, silicon, germanium) have extremely high dielectric constants. For these materials, AR-coatings are needed to minimize reflection losses. This can be done by coating both window surfaces with a material of thickness $\lambda/4$ and refractive index $n_{AR} = \sqrt{n}$. Coatings with the required dielectric constants are very rare. Unfortunately, most of them have poor transparency in the THz frequency range (e.g. PE, Parylene, Teflon) leading to high absorption losses. Precisely manufactured HDPE windows are only slightly worse than a Parylene coated silicon window (for example) in the THz range (1). In addition, AR-coatings are not always easily applicable to the window substrate. Especially in the case of cryogenic temperatures, glued or sintered materials may peal off under temperature cycling. Fig. 1 gives an overview of appropriate THz window designs.

A second method to match the impedance of the window material to free space is to design artificial dielectrics with a refractive index of $\sqrt{n}$ by cutting a well defined topology of $\lambda/4$ depth into the substrate. The generated dielectric constant is a function of the filling factor and can be calculated. Theories for 1D structures like rectangular-, multistep-, triangular- and sin-wave-grooves [1][2] and 2D structures like rectangles and holes [3]. are known. For wavelengths up to 400 GHz, grooved HDPE can be fabricated with common manufacturing techniques such as CNC milling. However, the needed sub-wavelength structures of about 6 microns at 1.9 THz are quite difficult to manufacture conventionally.

Rectangular grooves were manufactured into high resistivity silicon by using the Bosch-process to keep the fabrication process simple and to get high transmission at THz frequencies.

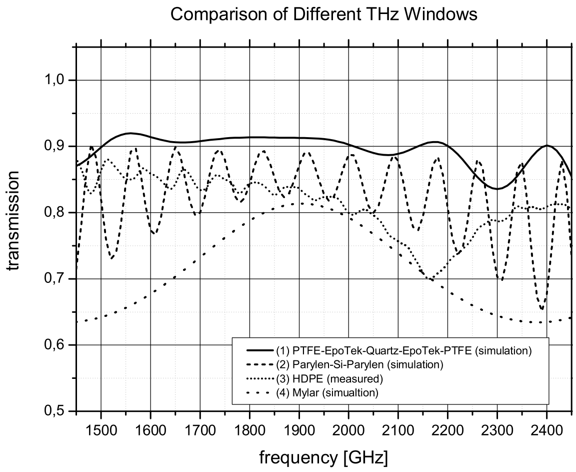

Fig. 1. (1) Theoretical transmission of PTFE glued on z-cut crystal quartz: $25\mu m$ PTFE, $5\mu m$ Epo-Tek-301, $500\mu m$ quartz, $5\mu m$ Epo-Tek-301 and $25\mu m$ PTFE. (2) Calculation for Parylene coated silicon: $24.38\mu m$ Parylene, $527\mu m$ silicon and $24.38\mu m$ Parylene. (3) Measured (FTS - Bruker) transmsission of $1.29mm$ HDPE. (4) Simulated data of $90\mu m$ Mylar.

II. Theory

Theories to calculate 1D or 2D AR-structures are given by [1][2] and [3]. In both cases, the topology models the dielectric constant of the substrate, thus artificial dielectrics can be designed. It should be noted, that 1D structures are polarisation dependent and birefringent [4], whereas 2D structures are not.

Raguin et al. [1] developed the 2nd order effective medium theory (EMT), which allows the calculation of the dielectric constant of rectangular grooves as a function of the filling factor $f = b/p$ (see Fig. 2). The groove geometry is defined as shown in Fig. 3.

The groove depth d equals a quarter wavelength of the incident wave (λ_0) in the window material:

$$d = \frac{\lambda_0}{4\sqrt{n_s}} \qquad (1)$$

The grating equation sets an upper bound on the period-to-wavelength ratio, since the 2nd order EMT is only valid as long as only the zeroth diffraction order propagates:

$$\frac{p}{\lambda_0} \leq \frac{1}{\beta(n_s + n_i)} \qquad (2)$$

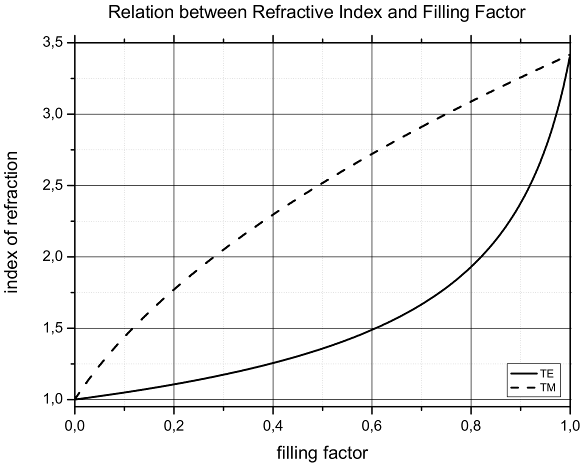

Fig. 2. Dependency between the filling factor and the resulting refractive index for an incident TE and TM wave. For calculation of $n(f)$ see [1]

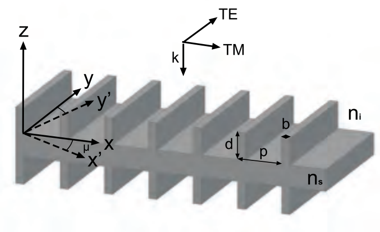

Fig. 3. Rectangular grooves as an example of a polarization dependent 1D-structure matching the impedance of the substrate with refractive index n_s to free space (n_i). Groove pitch p, depth d and tooth width b. The incident wave propagates in k-direction with rotation angle μ with respect to the groove pitch vector.

The design constant β, describes how much smaller the ratio p/λ_0 is than the critical value $1/(n_s + n_i)$. For ease of manufacturing β should be close to unity. Values of β less than unity allow the propagation of higher diffraction orders, hence 2nd order EMT fails.

III. SIMULATION

Simulation of the artificial dielectric is possible by using a simple transmission line analogue (Fig. 4), as long as $\beta \geq 1$ for any wavelength in a given frequency range, angle $\mu = 0°$ and the k-vector is perpendicular to the surface.

The transmission line method can not be properly used when β drops below 1 in the analyzed frequency band, because higher-order diffraction waves start to propagate. In this case the transmissivity should be calculated by solving Maxwell's Equations. Here, the FORTRAN-Code *Scatter*, written by R. Padman [5], is used. But a comparison of both simulation methods for a 1.9THz window shows, that the error introduced by the transmission line model is small for $\beta < 1$. At 2.075THz the error is only 1%, accompanied by a 10GHz frequency shift of the extremum (see Fig. 5). The error is a consequence of Eq. 2, since for the given period-to-wavelength ratio at 1.9THz, β drops under unity for frequencies greater than 1.9THz. At 2.075THz β decreases to ≈ 0.93. Identical simulation results are achievable if (for example) $\beta \geq 10$ at the design frequency.

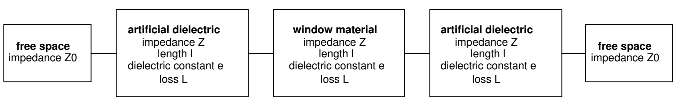

Fig. 4. Transmission line

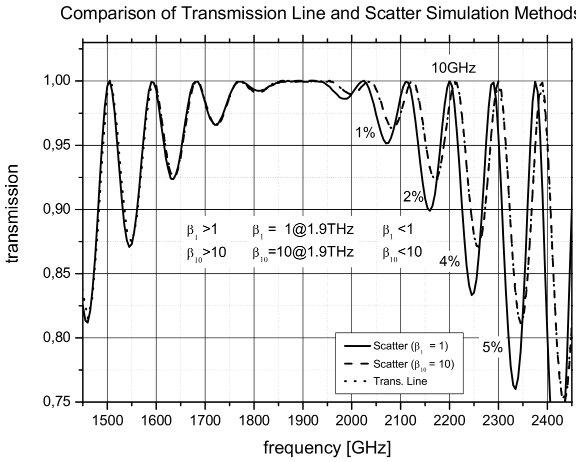

Fig. 5. Simulation of a grooved silicon ($n = 3.42$) window. Design frequency 1.9THz ($\lambda_0 = 158\mu m$). *Scatter*: $\beta_1 = 1$, i.e $p = 35.5\mu m$, $b = 6.5\mu m$ and $d = 21\mu m$ and $\beta_{10} = 10$, i.e. $p = 3.6\mu m$, $b = 0.8\mu m$ and $d = 21\mu m$. The maximum error using the transmission line analogue is only 2% within the band pass of 90% transmission.

The *Scatter* program also allows the computation of the transmission for different angles, μ. But as can be seen in Fig. 6, the groove orientation with respect to the E-field vector is not critical. Misalignment of $5°$ yields 3% loss only.

Much more critical is the groove depth. Taking Eq. 1 into account, one can see that the frequency of maximum transmission at a design frequency of 1.9THz is shifted by ≈ 80GHz per μm depth variation.

IV. DESIGN CONSTRAINTS

The KOSMA single pixel 1.9THz heterodyne HEB-receiver channel on GREAT, operated on the SOFIA airborne observatory, needs a low loss THz window, because observation time on the stratospheric telescope is expensive. Loss from the cryostat window should be as low as possible, no more than 10%. Due to safety reasons the window must support a pressure load of 3.5bar with a clear aperture of 25mm.

V. MEASUREMENTS

First, a stress analysis of a fixed mounted $527\mu m$ thick silicon wafer under a pressure load of 3.5bar at a clear aperture of 25mm was made. A subsequent single burst test approved

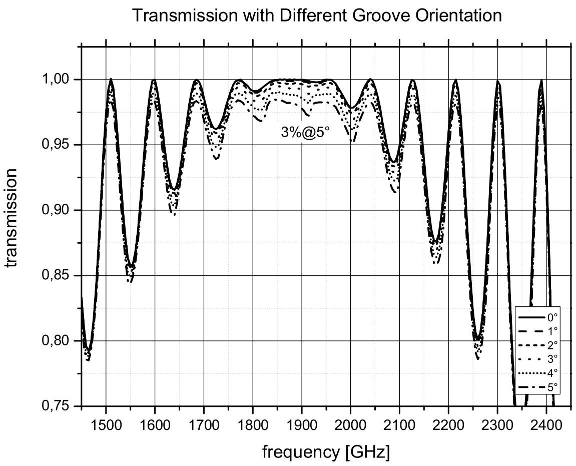

Fig. 6. Loss due to misalignment of the grooves with respect to the polarization vector of the incident wave (3% loss for $5°$ only!). *Scatter* simulation data with $\beta_1 = 1$, i.e $p = 35.5\mu m$, $b = 6.5\mu m$ and $d = 21\mu m$.

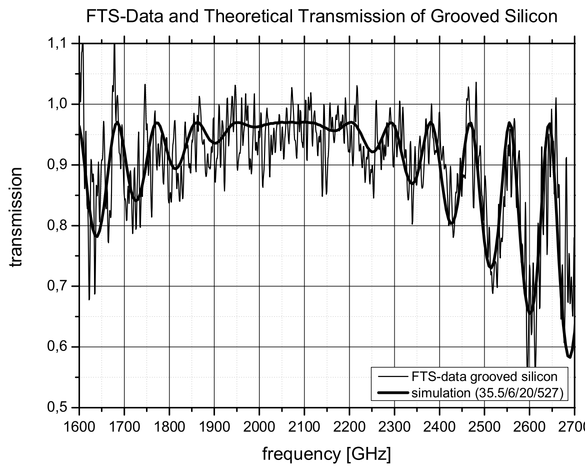

Fig. 8. Measured FTS data of our first dry-etched silicon cryostat window for THz-frequencies. Theoretically predicted transmission for a structure of b = 6m, p = 35.5m and d = 20m on 527m thick silicon is overlaid.

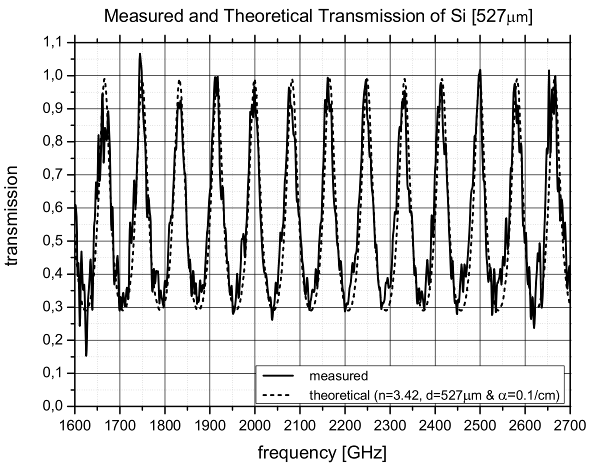

Fig. 7. FTS measurements yield a refractive index of $n = 3.42$ and an absorption of $0.1/cm$ for $3k\Omega cm$ silicon.

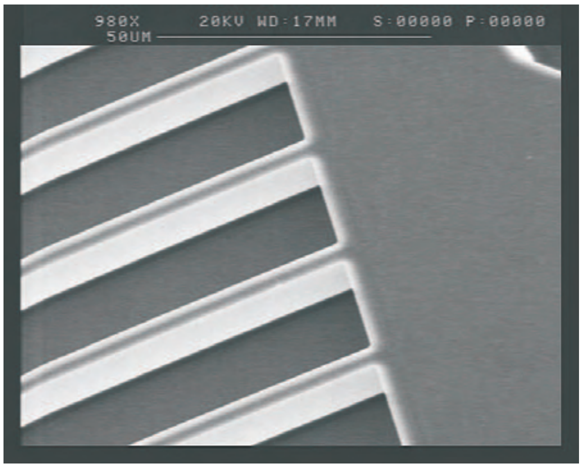

Fig. 9. SEM picture of our first low loss THz window. The rectangular groove AR-structure can be seen.

the preceding calculations and yielded a possible pressure load greater than 4bar.

In a next step, the refractive index and the absorption of high resistivity silicon was measured by using a Bruker FTS (see Fig. 7). The values obtained for the refractive index and absorption are $n_s = 3.42$ and $\alpha = 0.1/cm$, appropriate for the manufacture of a 1.9THz window with up to 98% transmittance, when reflective loss is minimized by a lossless AR-layer.

Based on the theory [1] a rectangular groove AR-structure for high resistivity silicon was calculated ($\beta = 1$ at 1.9THz: $p = 35.5\mu m$, $b = 6.5\mu m$ and $d = 21\mu m$). The transmission was simulated with the *Scatter* program. Then, the grooves were dry-etched by using the Bosch-process. The dry reactive ion etching process ensured the accuracy needed for the structure ($< 1\mu m$ for all dimensions) and kept the fabrication process simple. Fig. 8 shows fitted data ($p = 35.5\mu m$, $b = 6\mu m$ and $d = 20\mu m$) together with measured FTS data of our first device. As can be seen, maximum transmittance of more than 96% could be achieved. The 90% transmission bandwidth was found to be 400GHz. An SEM image of the etched grooves is shown by Fig. 9.

VI. Conclusion

Rectangular grooves, working as an AR-coating, were manufactured into high resistivity silicon ($3k\Omega cm$, $n = 3.42$ and $\alpha = 0.1/cm$). Silicon was used to keep the fabrication process simple (Bosch-process) and to get high transmission at THz frequencies. The topology was simulated by using a transmission line analogue and R. Padmans *Scatter* program. Theoretical predictions and FTS measurements of our first 1.9THz device are shown in Fig. 8. As can be seen, transmittance was found to be more than 96% at 2.1THz and the bandwidth within 90% transmission was 400GHz (1.9-2.3THz). The band pass shift to higher frequencies is a consequence of the etched groove depth, which is difficult to control. In addition, the etched tooth width b is a little bit smaller than calculated ($6\mu m$ instead of $6.5\mu m$), leading to a slightly different filling factor, hence to a smaller refractive index n_{AR} as needed for a perfect matching layer.

The mechanical design constraints, clear aperture of 25mm under a pressure load of 3.5bar, are satisfied. The result of a single burst test yields a possible pressure load greater than 4bar.

Acknowledgment

This work is supported by the *Deutsche Forschungsgemeinschaft* through grant SFB 494, and by the ministry of science of the state Nordrhein-Westfalen.

References

[1] D. Raguin and G. Morris, "Analysis of antireflection-structured surfaces with continous one-dimensional surface profiles," *Applied Optics*, vol. 32, no. 14, pp. 2581–2598, 1993.

[2] ——, "Antireflection structured surfaces for the infrared spectral region," *Applied Optics*, vol. 32, no. 7, pp. 1154–1167, 1993.

[3] S. Biber, J. Richter, S. Martius, and L. Schmidt, "Design of artificial dielectrics for anti-reflection-coatings," European Microwave Week. Munich, 2003.

[4] D. Mawet, J. Baudrand, C. Lenaerts, V. Moreau, P. Riaud, D. Rouan, and J. Surdej, "Birefringent achromatic phase shifters for nulling interferometry and phase coronagraphy," in *ESA SP-539: Earths: DARWIN/TPF and the Search for Extrasolar Terrestrial Planets*, 2003.

[5] R. Padman, *Program SCATTER - A Program for the Calcualtion of Plane-Wave Propagation in a Stratified Anisotropic Dielectric*, CSIRO Division of Radiophysics Internal Report RPP 2031(L), December 1976.

[6] C. Englert, M. Birk, and H. Maurer, "Antireflection coated, wedged, single-crystal silicon aircraft window for the far-infrared," *IEEE Transactions on Geoscience and Remote Sensing*, vol. 37, no. 4, pp. 1997–2003, 1999.

[7] H.-W. Hübers, J. Schubert, A. Krabbe, M. Birk, G. Wagner, A. Semenov, G. Gol'tsman, B. Voronov, and E. Gershenzon, "Parylene anti-reflection coating of a quasi-optical hot-electron-bolometric mixer at terahertz frequencies," *Infrared Physics and Technology*, vol. 42, pp. 41–47, 2001.

[8] M. Ji, C. Musante, S. Yngvesson, A. Gatesman, and J. Waldman, "Study of parylene as anti-reflection coating for silicon optics at THz frequencies." Proc. of the 11th Int. Symp. of Space THz Technol., 2000.

[9] R. Padman, *Program SCATTER for the Analysis of Dielectric Matching Layer*, National Radio Astronomy Observatory Charlottesville, Virginia, Electronic Division Technical Note No. 155, 1989.